British Journal of Pharmacology (2005) 145, 460–468
www.nature.com/bjp

Artocarpol A stimulation of superoxide anion generation in neutrophils involved the activation of PLC, PKC and p38 mitogen-activated PK signaling pathways

[1]Yu-Hsiang Kuan, [1,2]Ruey-Hseng Lin, [3]Lo-Ti Tsao, [4]Chun-Nan Lin & *[,3,5]Jih-Pyang Wang

[1]Institute of Medicine, Chung Shan Medical University, Taichung, Taiwan, Republic of China; [2]Department of Pharmacology, Chung Shan Medical University, Taichung, Taiwan, Republic of China; [3]Department of Education and Research, Taichung Veterans General Hospital, Taichung, Taiwan, Republic of China; [4]School of Pharmacy, Kaohsiung Medical University, Kaohsiung, Taiwan, Republic of China and [5]Graduate Institute of Pharmaceutical Chemistry, China Medical University, Taichung, Taiwan, Republic of China

1 Artocarpol A (ART), a natural phenolic compound isolated from *Artocarpus rigida*, stimulated a slow onset and long-lasting superoxide anion generation in rat neutrophils, whereas only slightly activated the NADPH oxidase in a cell-free system.

2 Pretreatment of neutrophils with pertussis toxin (1 $\mu g\,ml^{-1}$), 50 μM 2′-amino-3′-methoxyflavone (PD 98059), or 1 μM 1,4-diamino-2,3-dicyano-1,4-bis(2-aminophenylthio)butadiene (U0126) had no effect on ART-stimulated superoxide anion generation. ART (30 μM) did not induce extracellular signal-regulated kinase (ERK) phosphorylation.

3 4-(4-Fluorophenyl)-2-(4-methylsulfinylphenyl)-5-(4-pyridyl)-1*H*-imidazole (SB 203580) markedly attenuated the ART-stimulated superoxide anion generation (IC_{50} value of 4.3 ± 0.3 μM). Moreover, ART induced p38 mitogen-activated PK (MAPK) phosphorylation and activation.

4 The superoxide anion generation in response to ART was also substantially inhibited in a Ca^{2+}-free medium, and by pretreatment with 1 μM 1-[6-((17β-3-methoxyestra-1,3,5(10)-trien-17-yl)amino)-hexyl]-1*H*-pyrrole-2,5-dione (U-73122) and 100 μM 2-aminoethyldiphenyl borate (2-APB). ART (30 μM) stimulated the $[Ca^{2+}]_i$ elevation in the presence or absence of external Ca^{2+}, and also increased the D-*myo*-inositol 1,4,5-trisphosphate formation.

5 2-[1-(3-Dimethylaminopropyl)-1*H*-indol-3-yl]-3-(1*H*-indol-3-yl)-maleimide (GF 109203X) greatly inhibited the ART-stimulated superoxide anion generation (IC_{50} value of 7.8 ± 1.0 nM). ART increased the recruitment of PKC-α, -βI, and -βII to the plasma membrane of neutrophils, and stimulated Ca^{2+}-dependent PKC activation in the cytosol preparation.

6 ART induced the phosphorylation of $p47^{phox}$, which was attenuated by GF 109203X. Moreover, ART evoked the membrane association of $p47^{phox}$, which was inhibited by GF 109203X and SB 203580.

7 These results indicate that the ART stimulation of superoxide anion generation involved the activation of p38 MAPK, PLC/Ca^{2+}, and PKC signaling pathways in rat neutrophils.
British Journal of Pharmacology (2005) **145,** 460–468. doi:10.1038/sj.bjp.0706205
Published online 4 April 2005

Keywords: Artocarpol A; superoxide anion; intracellular free-Ca^{2+} concentration; mitogen-activated PK; PKC; neutrophils

Abbreviations: AA, arachidonic acid; 2-APB, 2-aminoethyldiphenyl borate; ART, artocarpol A; ERK, extracellular signal-regulated kinase; fluo3/AM, 1-[2-amino-5-(2,7-dichloro-6-hydroxy-3-oxo-3*H*-xanthen-9-yl)]-2-(2′-amino-5′-methylphenoxy)ethane-*N*,*N*,*N*′,*N*′-tetraacetic acid pentaacetoxymethyl ester; fMLP, formyl-Met-Leu-Phe; GF 109203X, 2-[1-(3-dimethylaminopropyl)-1*H*-indol-3-yl]-3-(1*H*-indol-3-yl)-maleimide; HBSS, Hanks' balanced salt solution; IP_3, D-*myo*-inositol 1,4,5-trisphosphate; MAPK, mitogen-activated PK; MBP, myelin basic protein; PD 98059, 2′-amino-3′-methoxyflavone; PMA, phorbol 12-myristate 13-acetate; SB 203580, 4-(4-fluorophenyl)-2-(4-methylsulfinylphenyl)-5-(4-pyridyl)-1*H*-imidazole; U0126, 1,4-diamino-2,3-dicyano-1,4-bis(2-aminophenylthio)-butadiene; U-73122, 1-[6-((17β-3-methoxyestra-1,3,5(10)-trien-17-yl)amino)hexyl]-1*H*-pyrrole-2,5-dione

Introduction

Neutrophils constitute the first line of host defense against the invasion of microorganisms through an array of microbicidal mechanisms including chemotaxis, phagocytosis, degranulation, and generation of reactive oxygen species, including superoxide anion and its toxic metabolites. The enzyme responsible for superoxide anion generation is NADPH oxidase. Inherited deficiencies of this enzyme result in chronic granulomatous disease, characterized by enhanced susceptibility to microbial infection (Smith & Curnutte, 1991). The mechanism of activation of superoxide anion generation in neutrophils is complex and incompletely understood. Upon neutrophils activation, the cytosol components of NADPH

*Author for correspondence at: Department of Education and Research, Taichung Veterans General Hospital, 160, Sec. 3, Chung-Kang Road, Taichung 407, Taiwan, Republic of China;
E-mail: w1994@vghtc.gov.tw
Published online 4 April 2005

oxidase ($p47^{phox}$, $p67^{phox}$, $p40^{phox}$, and Rac) are translocated to membrane and associated with the flavocytochrome b_{558}, which contains FAD and heme redox centers, to form a functional oxidase complex, which catalyzes the reduction of oxygen to superoxide anion by using NADPH as the electron donor (Segal & Abo, 1993). Phosphorylation of $p47^{phox}$, which induces a conformational change leading to the assembly of a functional oxidase, is a crucial step in oxidase activation (Babior *et al*., 2002). Previous reports demonstrated that the stimulation of neutrophils by receptor-binding ligands activates mitogen-activated PK (MAPK), including p38 MAPK and extracellular signal-regulated kinase (ERK, or p44/42 MAPK), during superoxide anion generation (El Benna *et al*., 1996). PLC is also activated by receptor-binding ligands, leading to the hydrolysis of $PI(4,5)P_2$ to generate D-*myo*-inositol 1,4,5-trisphosphate (IP_3), which increases in $[Ca^{2+}]_i$, and diacylglycerol, which activates PKC (Berridge, 1987). These two messengers act synergistically for superoxide anion generation.

The Moraceous plant *Artocarpus rigida* has been used as a folk veterinary remedy for the treatment of wounds in Asia. Artocarpol A (ART), a natural phenolic compound isolated from the root bark of this plant, was shown to inhibit phorbol 12-myristate 13-acetate (PMA)-induced superoxide anion generation in rat neutrophils and TNF-α formation in macrophage-like cell lines in our previous report (Chung *et al*., 2000). In this study, we found to our surprise that ART alone stimulates superoxide anion generation in rat neutrophils, and we herein describe the involvement of PLC/Ca^{2+}, PKC, and p38 MAPK signaling pathways in the ART-induced response by a combination of pharmacological and immunological approaches.

Methods

Isolation of neutrophils

Rat (Sprague–Dawley) blood was collected from the abdominal aorta and the neutrophils were purified by dextran sedimentation, centrifugation through Ficoll-Paque, and hypotonic lysis of erythrocytes (Wang *et al*., 1995). Purified neutrophils containing >95% viable cells were normally resuspended in Hanks' balanced salt solution (HBSS) containing 10 mM HEPES, pH 7.4, and 4 mM $NaHCO_3$, and kept in an icebath before use. All experiments in the present study were performed under the guidelines of the Institutional Experimental Laboratory Animal Committee and were in strict accordance with the Guide for the Care and Use of Laboratory Animals as adopted and promulgated by the U.S. National Institutes of Health.

Measurement of superoxide anion generation

Superoxide anion generation was determined by the superoxide dismutase-inhibitable reduction of ferricytochrome *c* (Wang *et al*., 1995). Briefly, the assay mixture contained neutrophils (2×10^6 cells) and 40 μM of ferricytochrome *c* in a final volume of 1.5 ml. The reference cuvette also received 17.5 U ml^{-1} of superoxide dismutase. Absorbance changes in the reduction of ferricytochrome *c* were monitored continuously at 550 nm in a double-beam spectrophotometer (Hitachi, U-3210).

Measurement of NADPH oxidase activity in a cell-free system

Neutrophils (1×10^8 cells ml^{-1}) were treated with 2.5 mM diisopropyl fluorophosphate and disrupted in Tris buffer (10 mM Tris–HCl, pH 7.0, 0.34 M sucrose, 10 mM benzamidine, and 2 mM phenylmethylsulfonyl fluoride) by sonication (Wang *et al*., 1997a). After centrifugation ($48{,}000 \times g$ for 45 min at 4°C), supernatants were pooled as the cytosolic fraction, and pellets were collected and resuspended in Tris buffer, as the membrane fraction. Plasma membrane and cytosolic fractions were mixed in 1.5 ml of assay buffer (0.17 M sucrose, 2 mM NaN_3, 1 mM $MgCl_2$, 1 mM EGTA, 65 mM KH_2PO_4–NaOH, pH 7.0) supplemented with 10 μM FAD, 3 μM GTPγS, 40 μM ferricytochrome *c*, 50 μM NADPH, and activated by 100 μM arachidonic acid (AA). Superoxide dismutase was present in the reference cuvette. Absorbance changes in the reduction of ferricytochrome *c* were monitored.

Immunoblot analysis of MAPK phosphorylation

After stimulation of cells (2×10^7 cells 0.5 ml^{-1}) with test drugs, the reactions were terminated by the addition of Laemmli sample buffer (Chang & Wang, 1999), and the solution was boiled for 5 min. Proteins (60 μg per lane) were resolved by 10% SDS–PAGE, and transferred to polyvinylidene difluoride membranes. The membranes were blocked with 5% (w v^{-1}) nonfat dried milk and probed with anti-phospho-p44/42 MAPK or anti-phospho-p38 MAPK. The blots were then stripped and reprobed with anti-pan ERK or anti-p38 MAPK antibody to standardize protein loading in each lane. Detection was performed with the enhanced chemiluminescence reagent. Quantification was by densitometry.

Measurement of p38 MAPK activity

Neutrophils (2×10^7 cells) were lysed on ice in 0.2 ml of lysis buffer (50 mM Tris–HCl, pH 7.5, 1 mM EDTA, 1 mM EGTA, 0.1% Triton X-100, 50 mM NaF, 10 mM sodium β-glycerophosphate, 5 mM sodium pyrophosphate, 0.1% 2-mercaptoethanol, 0.5 mM Na_3VO_4, 0.1 mM phenylmethylsulfonyl fluoride, and 1 μg ml^{-1} each of aprotinin, pepstatin, and leupeptin), and then clarified by centrifugation (Hsu *et al*., 2004). p38 MAPK in lysate was immunoprecipitated by the addition of rabbit polyclonal anti-p38 MAPK and 50% slurry of protein A-Sepharose beads, and the samples were rotated at 4°C overnight. The beads were washed twice in lysis buffer and once in kinase assay buffer (40 mM HEPES, pH 7.4, 10 mM $MgCl_2$, 10 mM $MnCl_2$, 1 mM Na_3VO_4, and 2 mM dithiothreitol). The kinase activity of p38 MAPK was assayed using 10 μg of myelin basic protein (MBP) as substrate and 200 μM ATP in an assay volume of 20 μl, which was incubated at 30°C for 20 min. The reaction was stopped by the addition of Laemmli sample buffer and the solution was boiled for 5 min. Proteins were resolved by 12.5% SDS–PAGE, transferred to membranes, and probed with anti-phospho-MBP and p38 MAPK antibody. Detection was performed with the enhanced chemiluminescence reagent. Quantification was by densitometry.

Measurement of $[Ca^{2+}]_i$

Neutrophils (5×10^7 cells ml^{-1}) were incubated with 5 μM 1-[2-amino-5-(2,7-dichloro-6-hydroxy-3-oxo-3*H*-xanthen-9-yl)]-2-(2′-amino-5′-methylphenoxy)ethane-*N*,*N*,*N*′,*N*′-tetraacetic acid pentaacetoxymethyl ester (fluo-3/AM) for 45 min at 37°C. After being washed, the cells were resuspended in HBSS to 5×10^6 cells ml^{-1}. Fluorescence changes were monitored with a fluorescence spectrophotometer at 535 nM with excitation at 488 nm. $[Ca^{2+}]_i$ was calibrated from the fluorescence intensity as follows:

$$[Ca^{2+}]_i = K_d \times [(F - F_{min})(F_{max} - F)^{-1}]$$

where F is the observed fluorescence intensity. The values F_{max} and F_{min} were obtained at the end of experiments by the sequential addition of 0.33% Triton X-100 and 50 mM EGTA. The K_d was taken as 400 nM.

Determination of inositol phosphates

Neutrophils (3×10^7 cells ml^{-1}) were incubated with *myo*-[^{3}H]inositol (3,071 GBq mmol^{-1}) at 37°C for 2 h (Wang *et al*., 1997a). Cells were then washed twice with HBSS containing 10 mM LiCl. After stimulation of cells with test drugs, the reactions were stopped by addition of $CHCl_3 : CH_3OH$ (1 : 1, v v^{-1}) mixture and acidification with 2.4 M HCl. The aqueous phase was removed, neutralized with 0.4 M NaOH, and then applied to an AG 1-X8 resin (format) column. Inositol-1-phosphate, inositol bisphosphate, and IP_3 were eluted sequentially using 0.2, 0.4, and 1.0 M ammonium formate in 0.1 M formic acid, respectively, as eluents. Each of the column fractions was collected and counted in liquid scintillation counter.

Measurement of PKC and p47^{phox} membrane translocation

Neutrophils (5×10^7 cells) were disrupted in 0.3 ml Tris buffer supplemented with 10 μg ml^{-1} each of pepstatin and leupeptin by sonication. After removing the unbroken cells, the lysate was then further centrifuged (100,000 × *g* for 30 min at 4°C) to collect pellets as membrane fractions. Membrane proteins were resolved by 7.5 and 10% SDS–PAGE for PKC and p47^{phox}, respectively, and were transferred to polyvinylidene difluoride membranes. The polyvinylidene difluoride membranes were then probed with anti-PKC-α, anti-PKC-βI, anti-PKC-βII, or anti-p47^{phox} antibody, and also with anti-CD88 antibody to standardize protein loading in each lane. Detection was performed with the enhanced chemiluminescence reagent. Quantification was by densitometry.

Measurement of PKC activity

Neutrophils (5×10^7 cells) were suspended in 0.5 ml of buffer A (20 mM Tris–HCl, pH 7.5, 0.25 M sucrose, 50 mM 2-mercaptoethanol, 1 mM phenylmethylsulfonyl fluoride, 5 mM EDTA, 10 mM EGTA, and 0.01% leupeptin) and disrupted by sonication (Wang *et al*., 1995). After centrifugation (100,000 × *g* for 1 h at 4°C), the cytosolic fraction was removed. The kinase activity of PKC was assayed using 8 μg of MBP as substrate in an assay volume of 80 μl (50 μM ATP, 80 μg ml^{-1} of phosphatidylserine, 3 mM $MgCl_2$, 25 mM Tris–HCl, pH 7.5, cytosolic fraction as PKC source, and test drugs), which was incubated at 25°C for 30 min, in the presence of 5 mM $CaCl_2$. The reaction was stopped by the addition of Laemmli sample buffer and the solution was boiled for 5 min. Proteins were resolved by 15% SDS–PAGE, transferred to membranes, and probed with anti-phospho-MBP and anti-PKC-βI antibody. Detection was performed with the enhanced chemiluminescence reagent. Quantification was by densitometry.

Measurement of p47^{phox} phosphorylation

Neutrophils (2×10^7 cells) were suspended in 0.5 ml of lysis buffer (50 mM Tris–HCl, pH 8.0, 100 mM NaCl, 1 mM EDTA, 1 mM EGTA, 1% Nonidet P-40, 0.05% SDS, 0.5% sodium deoxycholate, 2 mM Na_3VO_4, 1 mM dithiothreitol, and 1 μg ml^{-1} each of aprotinin, pepstatin, and leupeptin) for 30 min at 4°C, and then clarified by centrifugation. The supernatants were removed and incubated with a specific anti-p47^{phox} antibody for 2 h at 4°C with constant mixing. Protein A-Sepharose was then added and incubated overnight at 4°C with constant mixing. The beads were sedimented and were washed twice in lysis buffer. After addition of Laemmli sample buffer, the solution was boiled for 5 min. Proteins were resolved by 10% SDS–PAGE, and immunoblot analysis with anti-phosphoserine antibody. The blots were then stripped and reprobed with anti-p47^{phox} antibody. Detection was performed with the enhanced chemiluminescence reagent. Quantification was by densitometry.

Materials

ART (purity >99%) was purified as previously described (Chung *et al*., 2000). Dextran T-500, *myo*-[^{3}H]inositol, and enhanced chemiluminescence reagent were purchased from Amersham Pharmacia Biotech (Buckinghamshire, U.K.). HBSS was obtained from Invitrogen (Carlsbad, CA, U.S.A.). 4-(4-Fluorophenyl)-2-(4-methylsulfinylphenyl)-5-(4-pyridyl)-1*H*-imidazole (SB 203580), 2-[1-(3-dimethylaminopropyl)-1*H*-indol-3-yl]-3-(1*H*-indol-3-yl)-maleimide (GF 109203X), 2′-amino-3′-methoxyflavone (PD 98059), calcein/AM, fluo-3/AM, 1,4-diamino-2,3-dicyano-1,4-bis(2-aminophenylthio)butadiene (U0126), 1-[6-((17β-3-methoxyestra-1,3,5(10)-trien-17-yl)amino)-hexyl]-1*H*-pyrrole-2,5-dione (U-73122), and 2-aminoethyldiphenyl borate (2-APB) were purchased from Calbiochem-Novabiochem (San Diego, CA, U.S.A.). Rabbit polyclonal antibodies to phospho-p44/42 MAPK and phospho-p38 MAPK were purchased from New England Biolabs (Beverly, MA, U.S.A.). Rabbit polyclonal antibodies to CD88, mouse polyclonal antibodies to p38 MAPK, and mouse monoclonal p47^{phox} antibody were obtained from Santa Cruz Biotechnology (Santa Cruz, CA, U.S.A.). Mouse monoclonal pan ERK antibody was purchased from BD Biosciences Pharmingen (San Diego, CA, U.S.A.). Mouse monoclonal phosphoserine antibody was purchased from Alexis (Carlsbad, CA, U.S.A.). Rabbit polyclonal antibodies to phospho-MBP was obtained from Upstate Biotechnology (Lake Placid, NY, U.S.A.). Polyvinylidene difluoride membrane was obtained from Millipore (Bedford, MA, U.S.A.). Other chemicals were purchased from Sigma-Aldrich (St Louis, MO, U.S.A.). The final percentage of dimethylsulfoxide (DMSO) in the reaction mixture was $\leqslant$0.5% (v v^{-1}).

Statistical analysis

Statistical analyses were performed using Student's *t*-test for two group comparisons test or ANOVA followed by the Bonferroni *t*-test for multigroup comparisons test; $P<0.05$ was considered significant for all tests. The curve estimation regression analysis with logarithmic model (SPSS) was used to calculate IC_{50} values.

Results and discussion

ART stimulated superoxide anion generation in neutrophil suspension and in a cell-free system

It is well documented that formyl-Met-Leu-Phe (fMLP) stimulates superoxide anion generation by binding to the G protein-coupled receptor. Several signaling pathways, initiated by receptor–ligand interaction, have been reported to be involved in the regulation of NADPH oxidase. Conversely, phorbol ester bypasses the membrane receptor, activates PKC directly (Castagna *et al*., 1982) and thus stimulates the superoxide anion generation. Exposure of neutrophils to ART evoked superoxide anion generation in a concentration-dependent manner (Figure 1a). Unlike fMLP, which stimulated a transient and rapid superoxide anion generation, ART and PMA induced a slow and long-lasting response, which was preceded by a lag. The finding that the ART-induced response was greatly diminished in the presence of diphenylene iodonium (DPI) (Figure 1b), the NADPH oxidase inhibitor (Cross & Jones, 1986), suggests that the superoxide anion generation was through the NADPH oxidase activation. Cell viability was $\geqslant 90\%$ during the incubation of cells with 30 μM ART at 37°C for 10 min as assessed in lactate dehydrogenase (LDH) release assay and in calcein fluorescence assay. These data imply that ART is probably not responsible for the anti-inflammatory effect of *A. rigida*, or alternatively that ART may exert its anti-inflammatory action through the inhibition of other biological functions of the inflammatory cells.

To determine whether ART directly stimulates NADPH oxidase activity, an experiment with NADPH oxidase in a cell-free system was performed. Addition of 100 μM AA to the mixture of neutrophil membrane and cytosolic fractions mimics the effect of phosphorylation of $p47^{phox}$ upon cell activation, and leads to the assembly and activation of NADPH oxidase (Fuchs *et al*., 1995). ART (30 μM) alone, however, only slightly evoked superoxide anion generation in the cell-free system (Figure 1c). It is plausible that ART acts via signaling-mediated mechanisms, while the direct stimulation of oxidase by ART might play a minor role in the superoxide anion generation in intact cells. Pretreatment of neutrophils with 1 $\mu g\,ml^{-1}$ of pertussis toxin, a $G_{i/o}$ protein inhibitor, for 90 min nearly abrogated the fMLP-induced superoxide anion generation but had no significant inhibitory effect on ART-induced response (data not shown), suggesting that the pertussis toxin-sensitive G protein is not linked to the effect of ART.

Role of ERK activation in ART-stimulated superoxide anion generation

Three distinct mammalian MAPKs have been identified: ERK (p44/42 MAPK), p38 MAPK, and c-Jun N-terminal kinase (JNK), each with different physiological roles. Cell activation induces a signaling cascade that leads to the activation of MAPK via phosphorylation of both tyrosine and threonine residues (Derijard *et al*., 1995). It has been reported that both ERK and p38 MAPK, but not JNK, phosphorylate $p47^{phox}$ (El Benna *et al*., 1996). To address the relevance of the ERK signal pathway to ART activation, we first examined the effect of the ERK signal blocker on ART-induced superoxide anion generation. U0126 and PD 98059, both MEK1/2 inhibitors (Favata *et al*., 1998), had no significant inhibition of fMLP- and ART-induced superoxide anion generation (Figure 2a). The role of ERKs in formyl peptide-stimulated superoxide anion generation is controversial (Avdi *et al*., 1996; Kuroki & O'Flaherty, 1997; Tamura *et al*., 1999). This variation may arise from the differences in experimental conditions. Nevertheless, the present results suggest that the ERK signaling pathway is not linked to ART-induced superoxide anion generation in rat neutrophils. Moreover, unlike fMLP, ART did not stimulate ERKs phosphorylation during the period of superoxide anion generation based on the immunoblot analysis with anti-phospho-p44/42 MAPK antibodies (Figure 2b). The absence

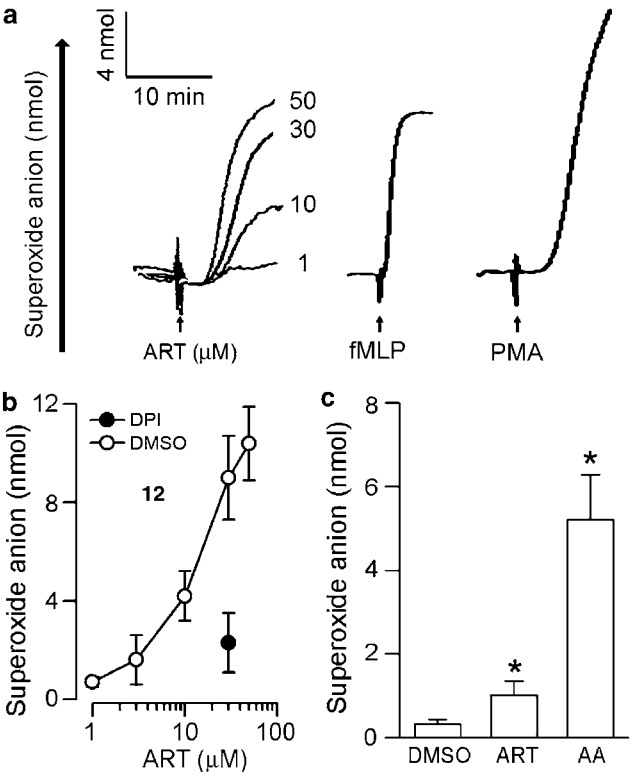

Figure 1 Stimulation of superoxide anion generation by ART. (a) Neutrophils were stimulated with the indicated concentrations of ART, 1 μM fMLP plus 5 $\mu g\,ml^{-1}$ of cytochalasin B, or 1 nM PMA. Superoxide anion generation was continuously monitored at 550 nm. Traces are representative of 3–4 independent experiments. (b) The concentration dependence of the superoxide anion generation by stimulaton with ART for 10 min is expressed as means ± s.d. of 4 independent experiments. In some experiments, cells were incubated with 1 μM diphenylene iodonium (DPI) for 3 min before stimulation with ART. (c) In a cell-free system, DMSO (as vehicle control), 30 μM ART, or 100 μM AA was added into the reaction mixture of cytosolic and membrane fractions. Values of superoxide anion generation are expressed as means ± s.d. of 4 independent experiments. $*P<0.05$, as compared with the vehicle control value.

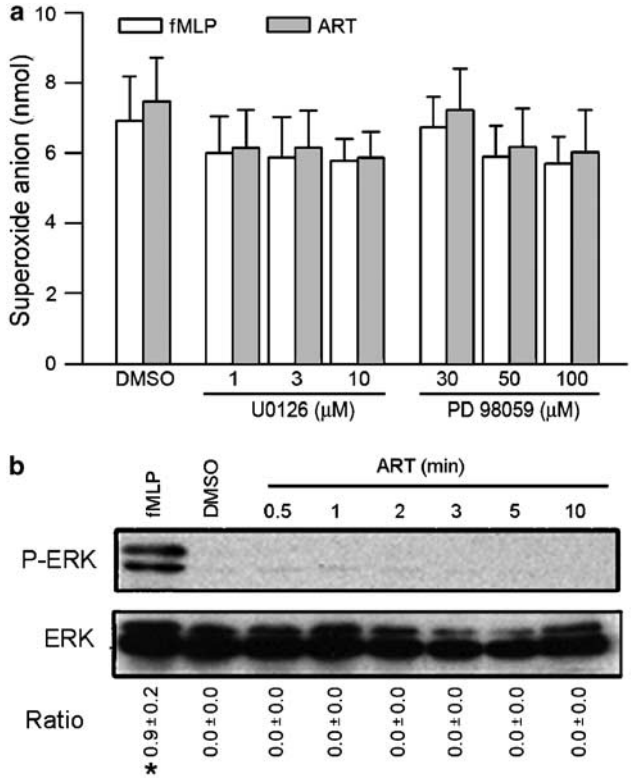

Figure 2 Effect of U0126 and PD 98059 on ART-stimulated superoxide anion generation, and the effect of ART on ERK phosphorylation. (a) Neutrophils were pretreated with DMSO, the indicated concentrations of U0126 or PD 98059 for 3 min at 37°C before stimulation with 30 μM ART or 1 μM fMLP plus 5 μg ml^{-1} of cytochalasin B for 10 min. Values are expressed as means ± s.d. of 6–8 independent experiments. (b) Neutrophils were incubated with DMSO, fMLP plus cytochalasin B for 1 min, or with ART for the indicated time. ERK phosphorylation was detected by immunoblot analysis using anti-phospho-p44/42 MAPK. The blots above were then stripped and reprobed with anti-pan ERK. The ratio of immunointensity between the ERK and the phosphorylation of ERK is shown. Values are expressed as means ± s.d. of 3–4 independent experiments. *$P<0.05$, as compared with the vehicle control value (lane 2).

of ERK phosphorylation in ART stimulation also points to an ERK-independent mechanism.

Role of p38 MAPK activation in ART-stimulated superoxide anion generation

Pretreatment of neutrophils with SB 203580, a p38 MAPK inhibitor (Cuenda *et al*., 1995), diminished the fMLP-stimulated superoxide anion generation, confirming a previous report (Zu *et al*., 1998), and also inhibited ART-induced response (IC_{50} value of 4.3 ± 0.3 μM) (Figure 3a). These results appear to reflect the involvement of the p38 MAPK signaling pathway. Furthermore, artocarpol stimulated p38 MAPK phosphorylation, as assessed by immunostaining with anti-phospho-p38 MAPK antibody, in a concentration- and time-dependent manner (Figure 3b). A significant increase in band immunointensity was observed at 10 μM ART for 10 min reaction time and at 30 μM ART for 4 min reaction time, which is compatible with the results of superoxide anion generation as shown in Figure 1a. Therefore, the immunoprecipitation of

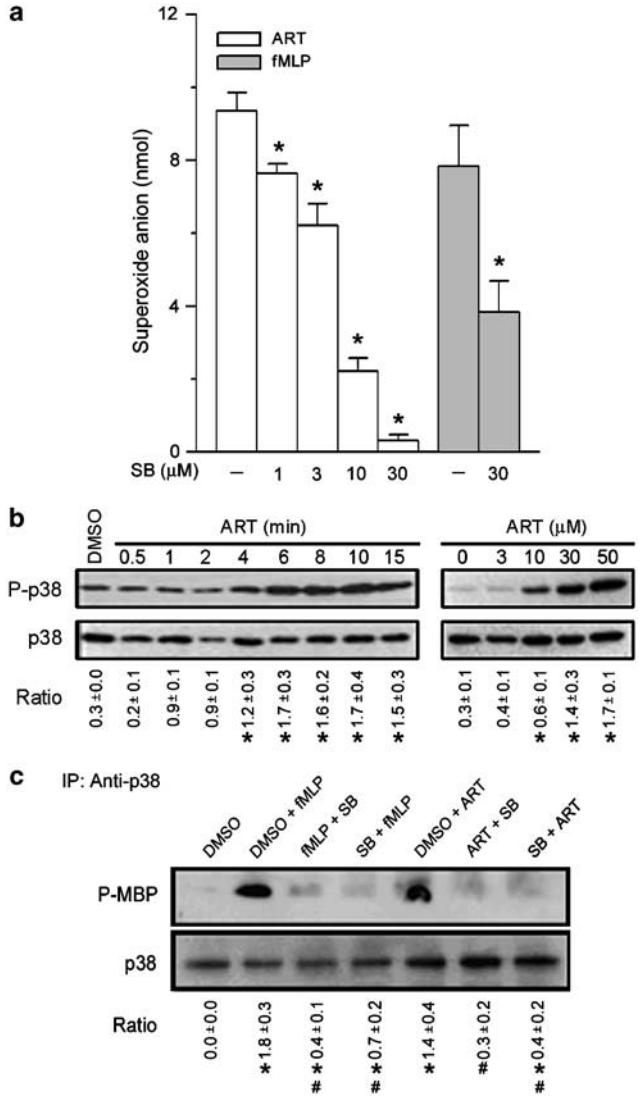

Figure 3 Effect of SB 203580 (SB) on ART-stimulated superoxide anion generation, and the effect of ART on p38 MAPK activation. (a) Neutrophils were pretreated with DMSO (as control) or the indicated concentrations of SB for 3 min at 37°C before stimulation with 30 μM ART or 1 μM fMLP plus 5 μg ml^{-1} of cytochalasin B for 10 min. Values are expressed as means ± s.d. of 3–5 independent experiments. *$P<0.05$, as compared with the corresponding control values. (b) Cells were incubated with DMSO, 30 μM ART for the indicated time or with the indicated concentrations of ART for 10 min. The ratio of immunointensity between the p38 MAPK and the phosphorylation of p38 MAPK is shown. Values are expressed as means ± s.d. of 3–4 independent experiments. *$P<0.05$, as compared with the vehicle control value (lane 1). (c) Cells were preincubated with DMSO or 30 μM SB for 3 min before stimulation with fMLP plus cytochalasin B for 1 min (SB + fMLP) or with ART for 10 min (SB + ART). Cell lysates were immunoprecipitated with anti-p38 MAPK antibody, and assayed for MAPK activity using MBP as substrate. In some experiments, the cell lysates from fMLP- or ART-activated cells were immunoprecipitated with anti-p38 MAPK antibody, and assayed for MAPK activity in the presence of SB (fMLP + SB or ART + SB). The ratio of immunointensity between the p38 MAPK and the phosphorylation of MBP is shown. Values are expressed as means ± s.d. of 3–4 independent experiments. *$P<0.05$, as compared to the vehicle control value (lane 1); $^{\#}P<0.05$, as compared to the corresponding activated control values (lanes 2 and 5).

cell lysates of ART-stimulated cells with p38 MAPK-specific antibody and the kinase activity was assessed. Both fMLP and ART stimulated p38 MAPK activity (both $P<0.05$), which was greatly attenuated by SB 203580 (30 μM) treatment, at a concentration that greatly blocked superoxide anion generation, either before or after the immunoprecipitation of p38 MAPK (Figure 3c). It is likely that the p38 MAPK signaling pathway is implicated in ART-induced superoxide anion generation. There are at least four members of the p38 MAPK family, including p38 MAPK-α, -β, -γ, and -δ isoforms, in which p38 MAPK-α and -δ are expressed in neutrophils (Hale *et al*., 1999). SB 203580 inhibited p38 MAPK-α and -β, but not -γ and -δ (Wang *et al*., 1997b), implying that ART stimulated superoxide anion generation via p38 MAPK-α activation.

Role of the PLC/Ca^{2+} signaling pathway in ART-stimulated superoxide anion generation

It is conceivable that the PLC/Ca^{2+} signal pathway is implicated in fMLP-induced superoxide anion generation. Like fMLP, the ART-induced response was nearly abrogated in a Ca^{2+}-free medium (Figure 4a). Thus, we sought to determine whether the PLC/Ca^{2+} signal pathway could be involved. The finding that U-73122 (1 μM), an inhibitor of PLC-coupled processes, fully inhibited the fMLP- and ART-induced superoxide anion generation confirms this possibility. Moreover, a comparable inhibition was evident with 2-APB (100 μM), a cell-permeant IP_3 receptor blocker (Maruyama *et al*., 1997), providing further support for the notion (Figure 4a). Recent evidence indicates that the principal antagonistic effect of 2-APB is on Ca^{2+} entry rather than Ca^{2+} release (Bootman *et al*., 2002). Nevertheless, stimulation of superoxide anion generation by ART has been shown to be Ca^{2+}-dependent.

In fact, ART (30 μM), at effective concentration, stimulated a slow rate of $[Ca^{2+}]_i$ rise in a Ca^{2+}-containing medium, preceded by a 20–40 s lag, reached a maximal level at 1–1.5 min after stimulation, then gradually declined as assessed by the increase in fluo 3 fluorescence (Figure 4b, upper panel). Although the increase in $[Ca^{2+}]_i$ is neither sufficient nor always required for superoxide production, this messenger acts synergistically with other signals for superoxide anion generation. Cell activation causes an increase in $[Ca^{2+}]_i$ due to the release of Ca^{2+} from internal stores and/or an influx of Ca^{2+} across the plasma membrane. In the absence of external Ca^{2+}, ART stimulated a small $[Ca^{2+}]_i$ rise (Figure 4b, lower panel), suggesting that ART increased internal Ca^{2+} release and external Ca^{2+} entry.

The role of IP_3 in mediating Ca^{2+} release from internal stores is firmly established, but the mechanisms responsible for Ca^{2+} entry are less clear. The finding that U-73122 (10 μM) fully blocked the ART-induced Ca^{2+} rise implies the involvement of the PLC/IP_3 signal. This notion was further supported by the result that the exposure of *myo*-[^{3}H]inositol-loaded neutrophils to ART for 15 s significantly increased the IP_3 formation and this effect was inhibited by U-73122 (1 μM) (Figure 4c). The IP_3 formation coincided with the onset of $[Ca^{2+}]_i$ rise by ART. The mammalian PLC isoenzymes can be divided into four major families: PLC-β, -γ, -δ, and -ε (Rhee, 2001), which are regulated through different mechanisms. PLC-β2 has been reported to be the major PLC isoform in neutrophils (Li *et al*., 2000). However, a 10-fold higher

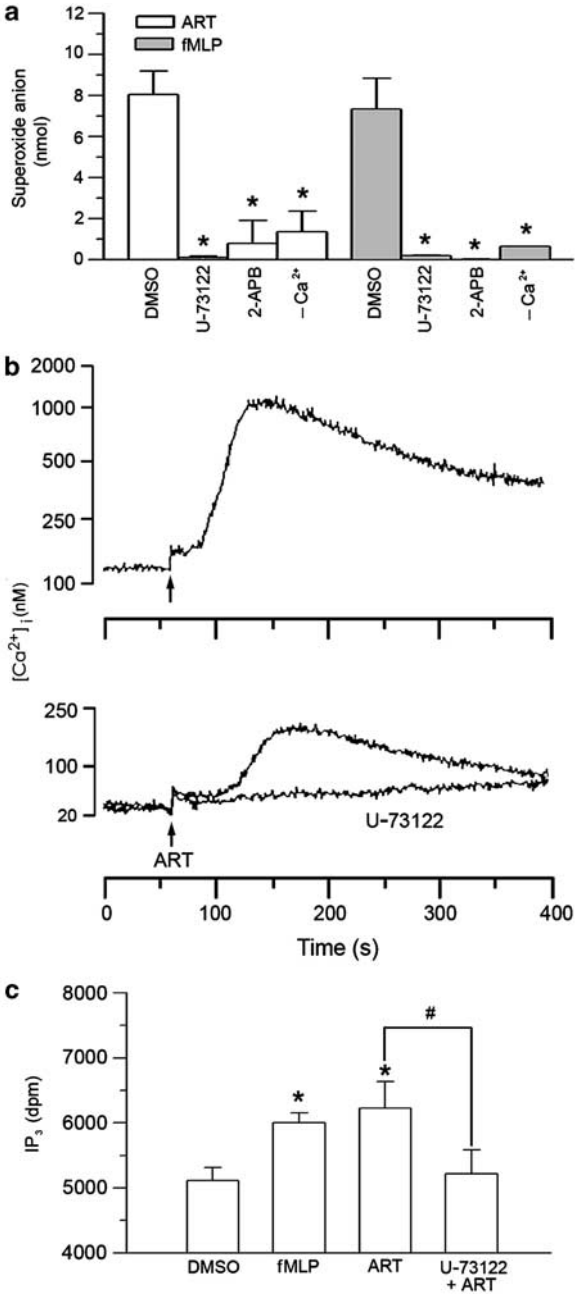

Figure 4 Effect of U-73122 and 2-APB on ART-stimulated superoxide anion generation, and the effect of ART on $[Ca^{2+}]_i$ changes and cellular IP_3 formation. (a) Neutrophils were pretreated with DMSO (as control), 1 μM U-73122, or 100 μM 2-APB in a Ca^{2+} (1 mM)-containing medium or with DMSO in a Ca^{2+}-free medium ($-Ca^{2+}$) for 3 min at 37°C before stimulation with 30 μM ART or 1 μM fMLP plus 5 μg ml^{-1} of cytochalasin B for 10 min. Values are expressed as means ± s.d. of 3–5 independent experiments. $^*P<0.05$, as compared with the corresponding control values. (b) Fluo-3-loaded cells were stimulated with ART (arrow) in a Ca^{2+} (1 mM)-containing medium (upper panel) or a Ca^{2+}-free medium (lower panel). In some experiments, cells were preincubated with 10 μM U-73122 for 1 min before stimulation with ART in a Ca^{2+}-free medium. The traces are representative of 3 independent experiments. (c) *Myo*-[^{3}H]inositol-loaded neutrophils were exposed to DMSO (as vehicle control) or fMLP for 10 s, or to ART for 15 s at 37°C. In some experiments, *myo*-[^{3}H]inositol-loaded cells were preincubated with 1 μM U-73122 for 1 min before stimulation with ART. The radioactivity of IP_3 generation was counted. Values are expressed as means ± s.d. of 5–6 independent experiments. $^*P<0.05$, as compared to the vehicle control value. $^{\#}P<0.05$.

concentration of U-73122 was required to diminish ART-induced Ca^{2+} release than the fMLP-induced Ca^{2+} response (Wang, 1996) and the ART-induced IP_3 formation. At present, we cannot clearly explain the difference in the U-73122 effects. One possibility is that a putative messenger other than IP_3 is probably also involved in ART-induced Ca^{2+} signals, which can be blocked by the higher concentration of U-73122, but this remains to be investigated.

Role of PKC activation in ART-stimulated superoxide anion generation

Based on the observation that ART stimulated the PLC/Ca^{2+} signaling pathway, we assumed the detection of PKC signals through the concomitantly generated diacylglycerol in ART-stimulated cells. Our previous report demonstrated that rat neutrophils express conventional isoforms (PKC-α and -β), novel isoforms (PKC-δ, -ε, and -θ), atypical isoforms (PKC-ι), and PKC-μ (Chang & Wang, 1999). Phosphorylation of $p47^{phox}$ *in vitro* is mediated by all families of PKC isoforms (Regier *et al*., 1999), although it is not known which specific isoform of PKC is responsible *in vivo*. It has been reported that the depletion of PKC-β inhibited fMLP-induced phosphorylation of $p47^{phox}$ and superoxide anion generation in differentiated HL-60 cells (Korchak *et al*., 1998), and neutrophils from PKC-β knockout mice markedly reduced the level of superoxide production (Dekker *et al*., 2000). Antisense-PKC-α-transfected THP-1 cells showed a decreased release of superoxide anion (Dieter & Schwende, 2000). Moreover, the requirement of PKC-δ in the regulation of NADPH oxidase activity in neutrophils has been reported recently (Brown *et al*., 2003). The respiratory burst caused by fMLP was inhibited by GF 109203X (0.1 μM), a broad PKCs inhibitor, in neutrophils (Tamura *et al*., 1999). The critical role of PKC in ART-induced response is supported by data that GF 109203X was potent against ART (IC_{50} value of 7.8 ± 1.0 nM) (Figure 5a).

In general, PKC activation is characterized by association of cytosolic PKC to the membrane fraction in intact cells. Since the ART stimulation of superoxide anion generation is via a Ca^{2+}-dependent mechanism, it is likely that the Ca^{2+}-independent PKC play a minor role. Therefore, immunoblot analysis was carried out to determine the subcellular distribution of Ca^{2+}-dependent PKC (α, βI, and βII). Only a slight immunointensity for these PKC isoforms was detected in the membrane fractions of unstimulated cells. Addition of ART resulted in the membrane recruitment of PKCs in a time- and concentration-dependent manner (Figure 5b). A significant increase in band immunointensity of PKC-α was observed at 30 μM ART for 2 min reaction time, reached a maximal level at 7 min, and then declined, whereas the band intensity of PKC-βI increased at 5 min, reached a maximal level at 7 min and remained elevated to 10 min after stimulation. The band immunointensity of PKC-βII was reached a maximal level at 2 min after ART stimulation and remained elevated to 10 min at least. The kinetics of PKC activation is compatible with the results of superoxide anion generation as shown in Figure 1a,

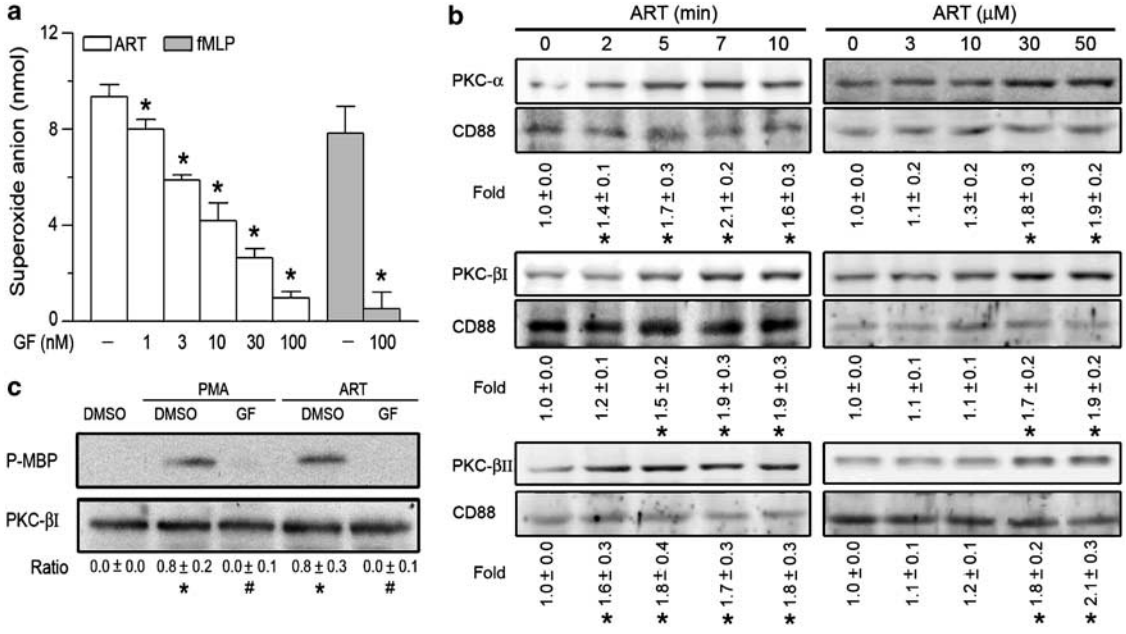

Figure 5 Effect of GF 109203X (GF) on ART-stimulated superoxide anion generation, and the effect of ART on PKC activation. (a) Neutrophils were pretreated with DMSO (as control) or the indicated concentrations of GF for 3 min at 37°C before stimulation with 30 μM ART or 1 μM fMLP plus 5 μg ml^{-1} of cytochalasin B for 10 min. Values are expressed as means ± s.d. of 3–4 independent experiments. $^*P<0.05$, as compared with the corresponding control values. (b) Neutrophils were treated with 30 μM ART for the indicated time or with the indicated concentrations of ART for 7 min at 37°C. The membrane-associated PKC was immunoblotted with the specific monoclonal antibody to PKC-α, -βI, or -βII. The polyvinylidene difluoride membranes were also probed with anti-CD88 antibody as the loading control. The fold increase in the immunointensity as compared with the corresponding control values (lane 1) is shown. Values are expressed as means ± s.d. of 6–7 independent experiments. $^*P<0.05$, as compared with the corresponding control values. (c) Cytosolic PKC was incubated with DMSO or 0.1 μM GF for 3 min at 37°C before the addition of DMSO, 30 nM PMA or ART for 30 min at 25°C, using MBP as substrate. The ratio of immunointensity between the PKC-βI and the phosphorylation of MBP is shown. Values are expressed as means ± s.d. of 4 independent experiments. $^*P<0.05$, as compared with the vehicle control value (lane 1); $^{\#}P<0.05$, as compared with the corresponding activated control values (lanes 2 and 4).

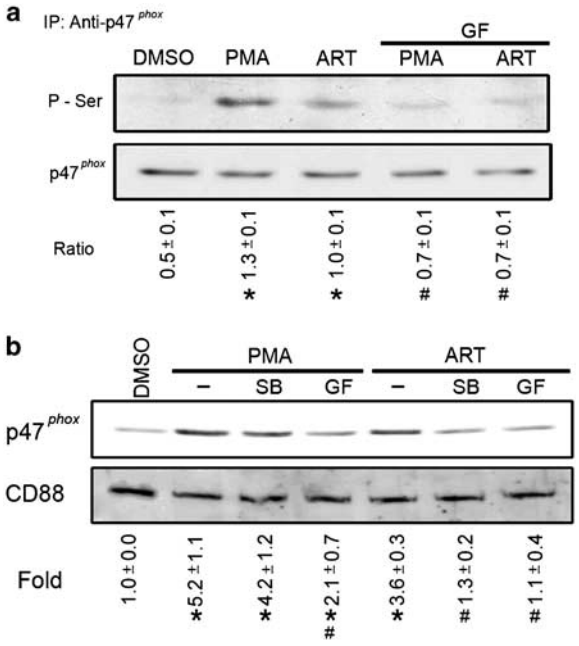

Figure 6 ART stimulated the phosphorylation of p47^{phox} and the translocation of p47^{phox} to the plasma membrane. (a) Neutrophils were treated with DMSO or 0.1 μM GF109203X (GF) for 3 min at 37°C before stimulation or no stimulation with 30 μM ART or 2 μM PMA for 10 min. The p47^{phox} in cell lysates were immunoprecipitated with a specific antibody to p47^{phox}. Phosphorylation of p47^{phox} was detected by immunoblot analysis using anti-phosphoserine antibody. The blots above were then stripped and reprobed with anti-p47^{phox} antibody. The ratio of immunointensity between the p47^{phox} and the phosphorylation of p47^{phox} is shown. Values are expressed as means ± s.d. of 3–4 independent experiments. $^{*}P<0.05$, as compared with the vehicle control value (lane 1); $^{\#}P<0.05$, as compared with the corresponding activated control values (lanes 2 and 3). (b) Neutrophils were treated with DMSO, 30 μM SB 203580 (SB) or GF for 3 min at 37°C before stimulation with ART or PMA for 10 min. The membrane-associated p47^{phox} was immunoblotted with anti-p47^{phox} antibody. The polyvinylidene difluoride membranes were also probed with anti-CD88 antibody as the loading control. The fold increase in the immunointensity as compared with the vehicle control value (lane 1) is shown. Values are expressed as means ± s.d. of 6–7 independent experiments. $^{*}P<0.05$, as compared with the vehicle control value; $^{\#}P<0.05$, as compared with the corresponding activated control values (lanes 2 and 5).

supporting the possibility that PKC regulates ART-induced response. Moreover, that the superoxide anion generation in response to ART stimulation in cells was accompanied by an increase in PKC activation is further supported by the observation that the addition of 30 μM ART significantly induced cytosolic PKC activation in the presence of Ca^{2+} (Figure 5c), which was fully inhibited by 0.1 μM GF 109203X. Pretreatment of cells with ART desensitized the PKC activation stimulated by the subsequent addition of PMA that may account for the inhibition of PMA-induced superoxide anion generation in our previous report (Chung *et al*., 2000).

ART stimulates the phosphorylation of p47^{phox} and the translocation of p47^{phox} to the plasma membrane

Stimulation of neutrophils by fMLP and phorbol ester results in extensive phosphorylation of p47^{phox} (DeLeo *et al*., 1999). p47^{phox} is phosphorylated on multiple sites through the action of several serine/threonine kinases including PKC, MAPK, p21^{rac}-activated PK, and a novel phosphatidic acid-activated PK (El Benna *et al*., 1996; Regier *et al*., 1999), resulting in a conformational rearrangement, exposing SH3 domain, proline-rich regions, and a PX domain those together mediate interactions both with cytochrome b_{558} and p67^{phox} (Lambeth, 2000). Thus, p47^{phox} appears to serve as an adaptor protein, providing a platform for the assembly of a functional oxidase. Like PMA, ART (30 μM) induced the serine phosphorylation of p47^{phox} (Figure 6a), which was attenuated by 0.1 μM GF 109203X, implying the participation of PKC signaling. Moreover, ART evoked the membrane association of p47^{phox} (Figure 6b), which was inhibited by GF 109203X and 30 μM SB 203580, whereas the 2 μM PMA-induced translocation of p47^{phox} to the plasma membrane was suppressed by GF 109203X but not by SB 203580. These data imply the involvement of PKC and p38 MAPK signaling in ART-stimulated recruitment of p47^{phox} to membrane. Previous reports demonstrated that SB 203580 did not prevent the fMLP-induced translocation of p47^{phox}/p67^{phox} to the plasma membrane of neutrophils (Lal *et al*., 1999) but inhibited that of the serum-opsonized zymosan (OZ)-induced response (Yamamori *et al*., 2002).

In conclusion, ART stimulates superoxide anion generation in rat neutrophils probably through the activation of p38 MAPK, PLC/Ca^{2+}, and PKC signaling pathways to promote the phosphorylation of p47^{phox} and the assembly of the NADPH oxidase in the plasma membrane, which leads to release of the superoxide anion to the extracellular compartment. The direct activation of NADPH oxidase may play a minor role in the ART-induced response.

This study was supported in part by grants from the National Science Council (NSC-91-2320-B-075A-004) and Taichung Veterans General Hospital (TCVGH-927303C), Taiwan, Republic of China.

References

AVDI, N.J., WINSTON, B.W., RUSSEL, M., YOUNG, S.K., JOHNSON, G.L. & WORTHEN, G.S. (1996). Activation of MEKK by formyl-methionyl-leucyl-phenylalanine in human neutrophils. Mapping pathways for mitogen-activated protein kinase activation. *J. Biol. Chem.,* **271,** 33598–33606.

BABIOR, B.M., LAMBETH, J.D. & NAUSEEF, W. (2002). The neutrophil NADPH oxidase. *Arch. Biochem. Biophys.,* **379,** 342–344.

BERRIDGE, M.J. (1987). Inositol trisphosphate and diacylglycerol: two interacting second messengers. *Annu. Rev. Biochem.,* **56,** 159–193.

BOOTMAN, M.D., COLLINS, T.J., MACKENZIE, L., RODERICK, H.L., BERRIDGE, M.J. & PEPPIATT, C.M. (2002). 2-Aminoethoxydiphenyl borate (2-APB) is a reliable blocker of store-operated Ca^{2+} entry but an inconsistent inhibitor of $InsP_3$-induced Ca^{2+} release. *FASEB J.,* **16,** 1145–1150.

BROWN, G.E., STEWART, M.Q., LIU, H., HA, V.L. & YAFFE, M.B. (2003). A novel assay system implicates PtdIns(3,4)P_2, PtdIns(3)P, and PKCδ in intracellular production of reactive oxygen species by the NADPH oxidase. *Mol. Cell,* **11,** 35–47.

CASTAGNA, M., TAKAI, Y., KAIBUCHI, K., SANO, K., KIKKAWA, U. & NISHIZUKA, Y. (1982). Direct activation of calcium-activated, phospholipid-dependent protein kinase by tumor-promoting phorbol esters. *J. Biol. Chem.,* **257,** 7847–7851.

CHANG, L.C. & WANG, J.P. (1999). Examination of the signal transduction pathways leading to activation of extracellular signal-regulated kinase by formyl-methionyl-leucyl-phenylalanine in rat neutrophils. *FEBS Lett.,* **454,** 165–168.

CHUNG, M.I., KUO, H.H., YEN, M.H., LIN, C.N., YANG, S.Z., TSAO, L.T. & WANG, J.P. (2000). Artocarpol A, a novel constituent with potent anti-inflammatory effect, isolated from *Artocarpus rigida*. *Helv. Chim. Acta,* **83,** 1200–1204.

CROSS, A.R. & JONES, O.T. (1986). The effect of the inhibitor diphenylene iodonium on the superoxide-generating system of neutrophils: specific labeling of a component polypeptide of the oxidase. *Biochem. J.,* **237,** 111–116.

CUENDA, A., ROUSE, J., DOZA, Y.N., MEIER, R., COHEN, P., GALLAGHER, T.F., YOUNG, P.R. & LEE, J.C. (1995). SB 203580 is a specific inhibitor of a MAP kinase homologue which is stimulated by cellular stresses and interleukin-1. *FEBS Lett.,* **364,** 229–233.

DEKKER, L.V., LEITGES, M., ALTSCHULER, G., MISTRY, N., McDERMOTT, A., ROSE, J. & SEGAL, A.W. (2000). Protein kinase C-β contributes to NADPH oxidase activation in neutrophils. *Biochem. J.,* **347,** 285–289.

DELEO, F.R., ALLAN, L.A., APICELLA, M. & NAUSEEF, W.M. (1999). NADPH oxidase activation and assembly during phagocytosis. *J. Immunol.,* **163,** 6732–6740.

DERIJARD, B., RAINGEAUD, J., BARRETT, T., WU, I.H., HAN, J., ULEVITCH, R.J. & DAVIS, R.J. (1995). Independent human MAP-kinase signal transduction pathways defined by MEK and MKK isoforms. *Science,* **267,** 682–685.

DIETER, P. & SCHWENDE, H. (2000). Protein kinase C-α and -β play antagonistic roles in the differentiation process of THP-1 cells. *Cell. Signal.,* **12,** 297–302.

EL BENNA, J., FAUST, R.P., JOHNSON, J.L. & BABIOR, B.M. (1996). Phosphorylation of the respiratory burst oxidase subunit p47^{phox} as determined by two-dimensional phosphopeptide mapping. Phosphorylation by protein kinase C, protein kinase A, and a mitogen-activated protein kinase. *J. Biol. Chem.,* **271,** 6374–6378.

FAVATA, M.F., HORIUCHI, K.Y., MANOS, E.J., DAULERIO, A.J., STRADLEY, D.A., FEESER, W.S., VAN DYK, D.E., PITTS, W.J., EARL, R.A., HOBBS, F., COPELAND, R.A., MAGOLDA, R.L., SCHERLE, P.A. & TRZASKOS, J.M. (1998). Identification of a novel inhibitor of mitogen-activated protein kinase kinase. *J. Biol. Chem.,* **273,** 18623–18632.

FUCHS, A., DAGHER, M.C. & VIGNAIS, P.V. (1995). Mapping the domains of interaction of p40^{phox} with both p47^{phox} and p67^{phox} of the neutrophil oxidase complex using the two-hybrid system. *J. Biol. Chem.,* **270,** 5695–5697.

HALE, K.K., TROLLINGER, D., RIHANEK, M. & MANTHEY, C.L. (1999). Differential expression and activation of p38 mitogen-activated protein kinase α, β, γ, and δ in inflammatory cell lineages. *J. Immunol.,* **162,** 4246–4252.

HSU, M.F., LU, M.C., TSAO, L.T., KUAN, Y.H., CHEN, C.C. & WANG, J.P. (2004). Mechanisms of the influence of magnolol on eicosanoid metabolism in neutrophils. *Biochem. Pharmacol.,* **67,** 831–840.

KORCHAK, H.M., ROSSI, M.W. & KILPATRICK, L.E. (1998). Selective role for β-protein kinase C in signaling for superoxide anion generation but not degranulation or adherence in differentiated HL60 cells. *J. Biol. Chem.,* **273,** 27292–27299.

KUROKI, M. & O'FLAHERTY, J.T. (1997). Differential effects of a mitogen-activated protein kinase kinase inhibitor on human neutrophil responses to chemotactic factors. *Biochem. Biophys. Res. Commun.,* **232,** 474–477.

LAL, A.S., CLIFTON, A.D., ROUSE, J., SEGAL, A.W. & COHEN, P. (1999). Activation of the neutrophil NADPH oxidase is inhibited by SB 203580, a specific inhibitor of SAPK2/p38. *Biochem. Biophys. Res. Commun.,* **259,** 465–470.

LAMBETH, J.D. (2000). Regulation of the phagocyte respiratory burst oxidase by protein interactions. *Biochem. Mol. Biol. Int.,* **33,** 427–439.

LI, Z., JIANG, H., XIE, W., ZHANG, Z., SMRCKA, A.V. & WU, D. (2000). Roles of PLC-β2 and -β3 and PI3Kγ in chemoattractant-mediated signal transduction. *Science,* **287,** 1046–1049.

MARUYAMA, T., KANAJI, T., NAKADE, S., KANNO, T. & MIKOSHIBA, K. (1997). 2APB, 2-aminoethoxydiphenyl borate, a membrane-penetrable modulator of Ins(1,4,5)P_3-induced Ca^{2+} release. *J. Biochem. (Tokyo),* **122,** 498–505.

REGIER, D.S., WAITE, K.A., WALLIN, R. & McPHAIL, L.C. (1999). A phosphatidic acid-activated protein kinase and conventional protein kinase C isoforms phosphorylate p22^{phox}, an NADPH oxidase component. *J. Biol. Chem.,* **274,** 36601–36608.

RHEE, S.G. (2001). Regulation of phosphoinositide-specific phospholipase C. *Annu. Rev. Biochem.,* **70,** 281–312.

SEGAL, A.W. & ABO, A. (1993). The biochemical basis of the NADPH oxidase of phagocytes. *Trends Biochem. Sci.,* **18,** 43–47.

SMITH, R.M. & CURNUTTE, J.T. (1991). Molecular basis of chronic granulomatous disease. *Blood,* **77,** 673–686.

TAMURA, M., YOSHIDA, K. & KATAOKA, K. (1999). Guanosine 5′-*O*-(3-thiotriphosphate)-induced superoxide anion generation in permeabilized neutrophils requires protein kinase C and phospholipase C but not tyrosine kinase or phospholipase D. *Arch. Biochem. Biophys.,* **361,** 257–263.

WANG, J.P. (1996). U-73122, an aminosteroid phospholipase C inhibitor, may also block Ca^{2+} influx through phospholipase C-independent mechanism in neutrophil activation. *Naunyn-Schmiedeberg's Arch. Pharmacol.,* **353,** 599–605.

WANG, J.P., RAUNG, S.L., KUO, Y.H. & TENG, C.M. (1995). Daphnoretin induced respiratory burst in rat neutrophils is, probably, mainly through protein kinase C activation. *Eur. J. Pharmacol.,* **288,** 341–348.

WANG, J.P., TSAO, L.T., RAUNG, S.L., HSU, M.F. & KUO, S.C. (1997a). Inhibition by HAJ11 of respiratory burst in neutrophils and the involvement of protein tyrosine phosphorylation and phospholipase D activation. *Br. J. Pharmacol.,* **120,** 79–87.

WANG, X.S., DIENER, K., MANTHEY, C.L., WANG, S., ROSENZWEIG, B., BRAY, J., DELANEY, J., COLE, C.N., CHAN-HUI, P.Y., MANTLO, N., LICHENSTEIN, H.S., ZUKOWSKI, M. & YAO, Z. (1997b). Molecular cloning and characterization of a novel p38 mitogen-activated protein kinase. *J. Biol. Chem.,* **272,** 23668–23674.

YAMAMORI, T., INANAMI, O., SUMIMOTO, H., AKASAKI, T., NAGAHATA, H. & KUWABARA, M. (2002). Relationship between p38 mitogen-activated protein kinase and small GTPase Rac for the activation of NADPH oxidase in bovine neutrophils. *Biochem. Biophys. Res. Commun.,* **293,** 1571–1578.

ZU, Y.L., QI, J., GILCHRIST, A., FERNANDEZ, G.A., VAZQUE-ABAD, D., KREUTZER, D.L., HUANG, C.K. & SHA'AFI, R.I. (1998). p38 mitogen-activated protein kinase activation is required for human neutrophil function triggered by TNF-α or FMLP stimulation. *J. Immunol.,* **160,** 1982–1989.

(Received December 24, 2004
Revised January 28, 2005
Accepted February 17, 2005)